

***Aquilaria malaccensis* as a Green Corrosion Inhibitor for Mild Steel in HCl Solution**

Helen Lee Yun Sin^{1,2}, Minoru Umeda¹, Sayoko Shironita¹, Afidah Abdul Rahim^{2,*}, Bahruddin Saad²

¹ Department of Materials Science and Technology, Nagaoka University of Technology, 1603-1 Kamitomioka, 940-2188 Nagaoka, Niigata, Japan

² School of Chemical Sciences, Universiti Sains Malaysia, 11800 Pulau Pinang, Malaysia

*E-mail: afidah@usm.my

Received: 15 April 2016 / Accepted: 11 July 2016 / Published: 7 August 2016

The methanolic extract from the leaf of *Aquilaria malaccensis* was confirmed to inhibit the corrosion of mild steel in 1 mol dm⁻³ HCl based on gravimetric and electrochemical methods, and the leaf extract was found to inhibit corrosion by as much as 94.49 % at the concentration of 1500 ppm. The leaf extract acted as a mixed-type, but predominantly cathodic inhibitor for the potentiodynamic polarization measurement. The adsorption of the leaf extract on the surface of mild steel was by a mixed-type, but predominantly physisorption process, fitting the best into the Langmuir adsorption isotherm model. The surface morphology analysis revealed a less damaged surface when the leaf extract was added.

Keywords: *Aquilaria malaccensis*, corrosion inhibitor, mild steel, HCl

1. INTRODUCTION

There are several trees from the *Aquilaria* family that are farmed for harvesting the agarwood resin. *Aquilaria malaccensis* is an agarwood-producing tree naturally distributed in South and Southeast Asia [1]. These farmed trees are usually induced to produce the agarwood resin by inoculation, and the resin can be harvested from the woody parts of the tree such as the trunk, roots and the branches. The leaves have minor uses such as being sold as traditional teas for stomach ailments [2], but the leaves are usually thrown away in abundance as it is less profitable compared to the highly-prized resin.

Corrosion inhibitors are amongst the more popular methods for corrosion protection due to their cost-effectiveness. Although many effective synthetic inhibitors have been developed [3-7], the movement of the corrosion inhibition research has been geared towards greener approaches such as

using waste materials, especially from plants [8-10]. Aside from the likelihood that such inhibitors will be less toxic, it is also a more cost-saving approach as it is making use of waste materials as raw materials. The most acceptable mechanism of the corrosion inhibition from the plants is the adsorption of the extract's molecules, forming a protective thin film over the metals to create a barrier from the corrosive medium [11-13]. Many of the plants were reported to contain constituents that are helpful for the adsorption by physisorption (Van der Waals attraction), chemisorption (bond sharing) or a mix of both processes. The structure of the constituents mostly resembles those of the conventional organic inhibitors [13] with functional groups that are bond-sharing and/or electron-donating [14-17].

Aquilaria malaccensis has been previously reported for its good antioxidant properties and the existence of phytochemicals that could be beneficial as a corrosion inhibitor [18, 19]. Similarly, the *Aquilaria crassna* and *Aquilaria subintegra* leaf extracts have also been shown to successfully inhibit corrosion [20, 21]. The purpose of this paper is to clarify the corrosion inhibition mechanism of *Aquilaria malaccensis* for mild steel in 1 mol dm⁻³ HCl. The corrosion inhibition was studied by gravimetric and electrochemical methods and the adsorption isotherm model was used to explain the adsorption process. The scanning electron microscope (SEM) and electron dispersing x-ray spectroscopy (EDX) analyses were conducted in order to determine the surface morphology of the mild steel after corrosion.

2. METHODOLOGY

2.1. Extraction

The *Aquilaria malaccensis* leaf was obtained from Telok Kumbar, Penang Island, Malaysia. The collected mature leaves were wiped clean, air-dried, powdered and extracted. The powdered leaf was exhaustively extracted with methanol at room temperature (27 ± 2 °C) and concentrated using a rotary evaporator at 40 °C into a paste form. The paste was dried in an oven at 35 °C until no change in mass was observed.

2.2. Extract content analysis

The analysis of the present chemical constituents in the leaf extract was determined by a 6520 Accurate-Mass Q-TOF LC/MS by Agilent Technology (USA) using the methods as described by Helen et. al. [20]. 1000 parts per million (ppm) of the extract was prepared by diluting 1 mg of extract in 1 mL of 3% acetonitrile solution (97 % ultrapure water).

The separation was performed using an Agilent ZORBAX SB-C18 column. The MS and MS/MS analyses were carried out using positive mode electrospray ionization (ESI).

For the MS analysis, the dry gas temperature of 325 °C, gas flow rate of 5 L min⁻¹, nebulizer pressure of 30 psi and capillary voltage of 3500 V were used. The acquisition mode was set at the m/z range of 25-1700 with the scan rate of 1 spectra ms⁻¹.

For the MS/MS analysis, a collision energy of 20 eV was used. The other conditions were the same as the MS analysis.

2.3. Corrosion inhibition study

2.3.1. Solution and specimen

The 1 mol dm⁻³ HCl was prepared by diluting 37 % concentrated HCl (AR grade) in double distilled water. For solutions with the leaf extract, the leaf extract was diluted to specific concentrations (50 to 1500 ppm) using the prepared HCl solution then 50 mL of the solution was used for each specimen. Mild steel with the composition of: Fe; 99.146 %, C; 0.205%, Mn; 0.55%, Si; 0.06% and P; 0.039%, with the dimensions of 1 × 3 × 0.06 cm was used for the weight loss study while mild steel with an exposure area of 3.142 cm² was used for the electrochemical studies. The surface of the mild steel was successively polished with emery papers of grades from 200 to 1200 then degreased with acetone before it was rinsed with double distilled water. It was then lightly towel dried and left to dry at room temperature before it was used.

2.3.2. Weight loss method

The initial weight of the mild steel (1 × 3 × 0.06 cm) was measured then the mild steel was immersed into the HCl solutions with and without the presence of the leaf extract at various concentrations for 24 hours. It was then removed, rinsed with distilled water and dried before the final weight was measured. All the concentrations were evaluated in triplicate and the result was the mean of the triplicates. The experiment was performed at the room temperature of 27 ± 2 °C [21]. The inhibition efficiency (IE %) of the leaf extract was calculated using the following equation:

$$\text{IE \%} = \left(\frac{W_2 - W_1}{W_2} \right) \times 100 \quad (1)$$

where W_1 is the weight loss of the specimen immersed with the leaf extract (g) and W_2 is the weight loss of the blank specimen (g).

2.3.3. Electrochemical methods

All the electrochemical measurements were carried out using a Gamry Instruments Reference 600 (potentiostat/ galvanostat/ ZRA) with a three-electrode cell. Platinum was used as the counter electrode, a saturated calomel electrode (SCE) was used as the reference electrode and the mild steel was used as the working electrode. The open circuit potential (OCP) measurement was observed for 30 minutes before the electrochemical measurements were conducted. All the experiments were conducted at a temperature of 27 ± 2 °C [21].

2.3.3.1. Potentiodynamic polarization measurement

The measurement was conducted at the scan rate of 1 mVs⁻¹ at an overpotential of ± 300 mV with reference to the corrosion potential (E_{corr}). The linear segments of the anodic and cathodic curves

were extrapolated to E_{corr} to obtain the corrosion current densities (I_{corr}). The IE % of the leaf extract was calculated using the following equation:

$$\text{IE \%} = \left(\frac{I_2 - I_1}{I_2} \right) \times 100 \quad (2)$$

where I_1 is the current density of the specimen with the leaf extract ($\mu\text{A cm}^{-2}$) and I_2 is the current density of the blank specimen ($\mu\text{A cm}^{-2}$)

2.3.3.2. Electrochemical Impedance Spectroscopy (EIS)

The measurement was conducted at the frequencies from 100 k to 0.1 Hz at the amplitude of 10 mV and the scan rate of 10 points per decade. The fitting of the curves and the parameters were obtained using the Echem Analyst by Gamry. The IE % was calculated using the following equation:

$$\text{IE \%} = \frac{R_{\text{ct}(1)} - R_{\text{ct}(2)}}{R_{\text{ct}(1)}} \times 100 \quad (3)$$

where $R_{\text{ct}(1)}$ is the charge transfer resistance of the specimen with the leaf extract ($\Omega.\text{cm}^2$) and $R_{\text{ct}(2)}$ is the charge transfer resistance of the blank specimen ($\Omega.\text{cm}^2$)

2.3.3.3. Potential zero charge (PZC) analysis

The relation between the conductivity and the potential were studied with and without the extract (1500 ppm) in the range of $E_{\text{corr}} \pm 500$ mV with a voltage step value of 0.01 V and the AC voltage of 10 mV rms. The f_{max} of each specimen was obtained from its corresponding EIS measurement.

2.4. Surface analysis

The surface morphology of the mild steel was monitored using a FEI QUANTA PEG 60 - scanning electron microscope. The surface of the mild steel after 24 hours of immersion at room temperature of 26 ± 2 °C in the HCl solution with and without the leaf extract (at 1500 ppm) was analyzed by the SEM and EDX.

3. RESULTS AND DISCUSSION

3.1. Q-TOF LC/MS Analysis

Based on the Quadrupole-time of flight liquid chromatography/ mass spectrometry (Q-TOF LC/MS) analysis, the tentatively identified presence of ten constituents was obtained by matching the MS/MS of the leaf extract to those available from the METLIN Metabolite Database or to those generated using Mass FrontierTM 6.0. Out of the ten constituents, five were confirmed by using standards bought from Agros Organics and Sigma-Aldrich. The five confirmed constituents are choline, isoleucine, adenosine, phenylalanine and mangiferin. The other five tentatively identified constituents are tryptophan, iriflophenone 3,5-C-beta diglucoside, iriflophenone-3-C-beta glucoside,

12-oxo phytodienoic acid and genkwanin. The parameters of the constituents are as reported by Helen et al. [21] and Table 1 lists these examples.

Table 1. Constituents identified in *Aquilaria malaccensis* leaf extract produced by Q-TOF LC/MS

Tentative Identification	Rt (min)	[M-H] ⁺	major fragment ions m/z (% base peak)	MF
Adenosine	2.158	268.2338	136.0635	C ₁₀ H ₁₃ N ₅ O ₄
Iriflophenone 3,5-C-beta diglucoside	11.093	571.1671	433.1112, 469.1145, 403.1007, 355.0825, 367.0824, 457.115, 421.093, 379.0829, 397.0932	C ₂₅ O ₁₅ H ₃₀
Iriflophenone-3-C-beta glucoside	11.152	409.1155	195.0285, 313.0709, 231.0287, 219.0287, 271.06, 325.0708	C ₁₉ H ₂₀ O ₁₀
Mangiferin	11.83	423.0935	273.0415, 303.0524, 327.0524, 369.0628, 405.0841	C ₁₉ H ₁₈ O ₁₁

3.2. Weight loss method

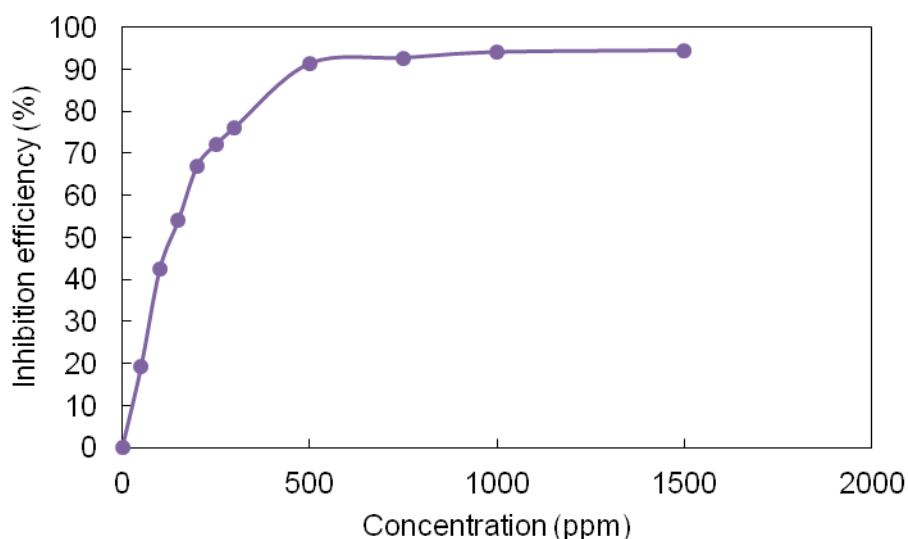


Figure 1. Weight loss measurement for mild steel in 1 mol dm⁻³ HCl with and without *Aquilaria malaccensis* leaf extract with immersion time of 24 hours done at the temperature of 27 ± 2 °C

The weight loss study was conducted at immersion time of 24 hours and room temperature of 27 ± 2 °C.

From Fig. 1, it was apparent that the increase in the concentration increased the inhibition efficiency of the leaf extract. The IE % increased until the concentration was 500 ppm, then the shape of the curve became a plateau at greater than 500 ppm. This indicated that the optimum IE % was

reached at the concentration of 500 ppm or higher for the weight loss method. The IE % continued to minimally increase after 500 ppm (91.33 %) until 1500 ppm (94.49 %).

3.3. Potentiodynamic polarization measurement

The potentiodynamic polarization measurement was realized in the $OCP \pm 300$ mV range from a cathodic-to-anodic sweep at the rate of 1 mVs^{-1} , at room temperature of 27 ± 2 °C and represented as Tafel plots in this paper. The obtained parameters listed are in Table 2. From Fig. 2, the current density (I_{corr}) of the Tafel curves decreased with the increase in the concentration of the leaf extract. The highest recorded IE % was 91 % at the concentration of 1500 ppm. The reaction when the cell was polarized to the cathodic region (more negative region) to the OCP is hydrogen evolution, the reaction of which can be simplified by the following ionic equation [22]:



while the reaction when the cell was polarized to the anodic region (more positive region) to the OCP is metal dissolution, the reaction of which can be simplified by the following ionic equation [22]:



While the leaf extract inhibited the cathodic reaction at all the tested concentrations, the anodic reaction was not inhibited at the lower concentrations.

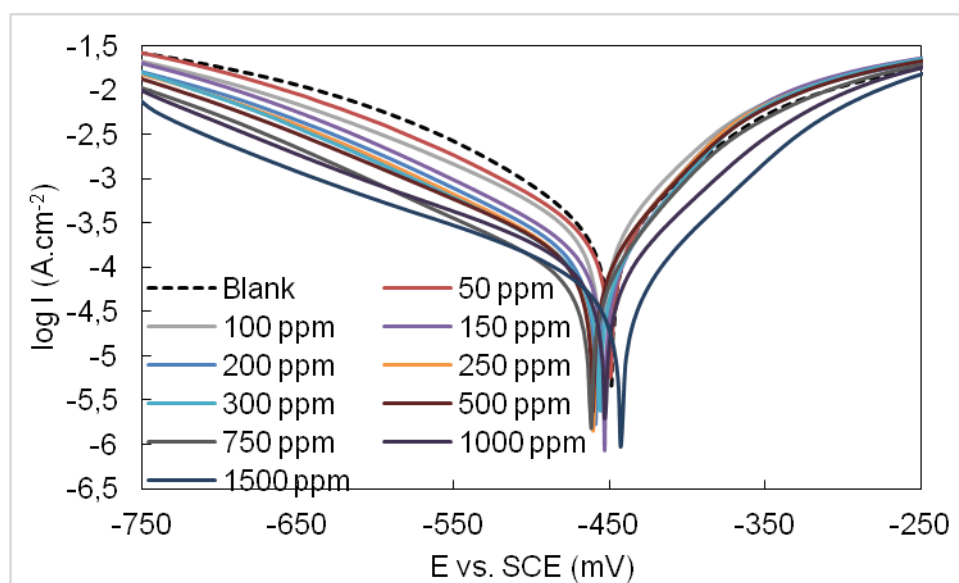


Figure 2. Tafel plot for mild steel in 1 mol dm^{-3} HCl with and without *Aquilaria malaccensis* leaf extract obtained at the scan rate of 1 mVs^{-1} and temperature of 27 ± 2 °C

However, the leaf extract successfully inhibited the anodic process at 750 ppm and higher as the current density was lowered in the anodic region. This indicated that the trigger for the inhibition effect happens at different concentrations of the leaf extract for the anodic and cathodic reactions. Both the anodic slope (β_a) and cathodic slope (β_c) were almost the same until 750 ppm then changed at

higher than 750 ppm. This indicated a change in the metal dissolution and hydrogen evolution at higher than 750 ppm. The E_{corr} of the leaf extract did not shift much from the E_{corr} of the blank specimen, indicating that the leaf extract acted as a mixed-type inhibitor at all concentrations [23]. However, since the current densities from the cathodic region were much lower than the anodic region, therefore, the leaf extract acted as a mixed-type but predominantly cathodic inhibitor.

Table 2. Parameters obtained from Tafel plot for mild steel in 1 M HCl with and without *Aquilaria malaccensis* leaf extract at the scan rate of 1 mVs^{-1} and temperature of $27 \pm 2 \text{ }^\circ\text{C}$

Concentration (ppm)	I_{corr} ($\mu\text{A}/\text{cm}^2$)	E_{corr} (mV)	β_a (mV/decade)	$-\beta_c$ (mV/decade)	IE %
blank	282	-449	75	117	-
50	200	-450	60	100	29
100	195	-456	56	113	31
150	126	-453	53	107	55
200	100	-459	41	101	65
250	89	-461	51	106	68
300	79	-456	51	109	72
500	76	-461	51	104	73
750	63	-462	52	118	78
1000	45	-453	58	137	84
1500	25	-443	63	147	91

3.4. Electrochemical impedance spectroscopy (EIS) measurement

The EIS measurements were conducted using the frequency range of 100 k to 0.1 Hz at the room temperature of $27 \pm 2 \text{ }^\circ\text{C}$ and represented by Nyquist plots in this paper (Fig. 3). For the EIS analysis, the curve had the shape of a single capacitive loop thus indicating the corrosion process to be mainly charge-transfer controlled for the metal dissolution. Supporting this fact are the slight changes in the n values with or without the presence of the leaf extract [24, 25]. The n values decreased with the increase in the concentration due to the adsorption of the extract molecules, thus increasing the nonhomogeneity of the surface [26, 27]. The curves appear to be in the shape of depressed semicircles, which is a deviation from the ideal capacitor behavior. Such deviations are characteristics of the dispersion in frequency due to the surface roughness and nonhomogeneities [28, 29]. Thus the Randles-CPE type equivalent circuit (Fig. 3 inset) was used to better fit the processes.

The impedance of CPE is expressed by:

$$Z_{\text{CPE}} = \frac{1}{Y_0(j\omega)^n} \quad (7)$$

where Y_0 is the frequency dependent magnitude of the pseudo-capacitance, j is $-1^{1/2}$, ω is the angular frequency and $-1 \leq n \leq 1$.

The parameters obtained from the Nyquist plot fitted into the Randles equation are listed in Table 3. While the solution resistance (R_s) values indicated slight changes, the charge transfer

resistance (R_{ct}) values evidently increased with the increase in the concentration. The R_{ct} was used to calculate the IE% using formula (3) and the leaf extract showed an increasingly successful corrosion inhibition with the increase in the concentration. The increase in the R_{ct} signifies a slow corroding system, and according to several papers, this is attributed to the adsorption of the leaf extract molecules that displace water molecules and other ions originally adsorbed on the surface of the mild steel, thus reducing the area of the active sites at which the corrosion takes place [24, 30, 31]. This may cause the formation of a protective thin film on the surface of the mild steel.

The lower CPE values for the leaf extract compared to the blank specimen could be caused by the reduction in the local dielectric constant and/or increase in the thickness of the electrical double layer. This could be due to the adsorption of the leaf extract molecules at the metal/solution interface [32].

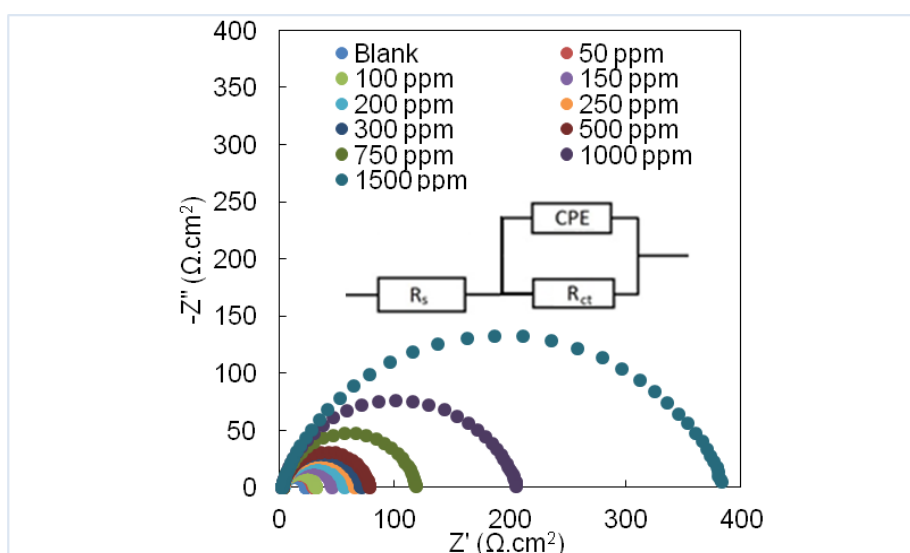


Figure 3. Nyquist plot for mild steel in 1 mol dm⁻³ HCl with and without *Aquilaria malaccensis* leaf extract, inset: Randles equivalent circuit model obtained using frequency range of 100 k to 0.1 Hz at temperature of 27 ± 2 °C

Table 3. Parameters obtained from Nyquist plot for mild steel in 1 M HCl with and without *Aquilaria malaccensis* leaf extract at frequency range of 100 k to 0.1 Hz and at temperature of 27 ± 2 °C

Concentration (ppm)	R_{ct} (Ω.cm ²)	R_s (Ω.cm ²)	CPE (μF/cm ²)	n	IE %
Blank	22.03	3.752	134	0.920	-
50	26.96	3.208	119	0.912	11.31
100	28.22	3.814	106	0.904	15.27
150	42.45	3.384	98	0.911	43.68
200	52.41	4.166	84	0.906	54.38
250	61.93	3.777	76	0.905	67.08
300	67.87	3.189	74	0.904	64.77
500	75.13	3.506	77	0.888	68.17
750	114.56	3.550	55	0.894	79.13
1000	199.39	3.214	67	0.855	88.01
1500	372.96	3.035	91	0.813	93.59

3.5 Adsorption isotherm model

The corrosion retarding effect observed for all the corrosion measurements was due to the adsorption of the inhibitor molecules on the surface in the form of a protective thin film from the aggressive acid solution while the exposed areas of the surface of the mild steel undergo the corrosion process. Thus, the assumption is made that the inhibition efficiency is directly related to the surface of the mild steel that is ‘covered’/adsorbed by the inhibitor’s molecules [33]. To understand the type of adsorption by the leaf extracts’ molecules on the surface of the mild steel, the surface coverage (Θ) calculated from the different corrosion measurement methods ($\Theta = IE \% / 100$) was fitted into several adsorption isotherm models. The Langmuir adsorption isotherm was best fit with a coefficient of determination (R^2) value of close to unity.

The Langmuir adsorption isotherm model assumes that the adsorbed molecules form a monolayer of film, only occupy one site and do not interact with other molecules [34, 35]:

$$\frac{c}{\Theta} = \frac{1}{K_{ads}} + c \tag{8}$$

where C is the concentration, Θ is the surface coverage, and K_{ads} is the adsorption constant

Plotting C/Θ versus C yields Fig. 4.

The K_{ads} value is related to the Gibbs free energy [36]:

$$\Delta G_{ads} = -RT \ln (K_{ads} \times A) \tag{9}$$

where ΔG_{ads} is the change in the Gibbs free energy/standard adsorption free energy, R is the universal gas constant ($8.314 \text{ J K}^{-1} \text{ mol}^{-1}$), T is the absolute temperature (K), and A is the density of water (1000 g L^{-1})

There are two main types of adsorptions: i.e., physisorption and chemisorption. The physisorption process, which is indicated by the values of ΔG_{ads} less negative than -20 kJ mol^{-1} , is attributed to the electrostatic interaction between a charged surface of the substrate and the ions in the medium.

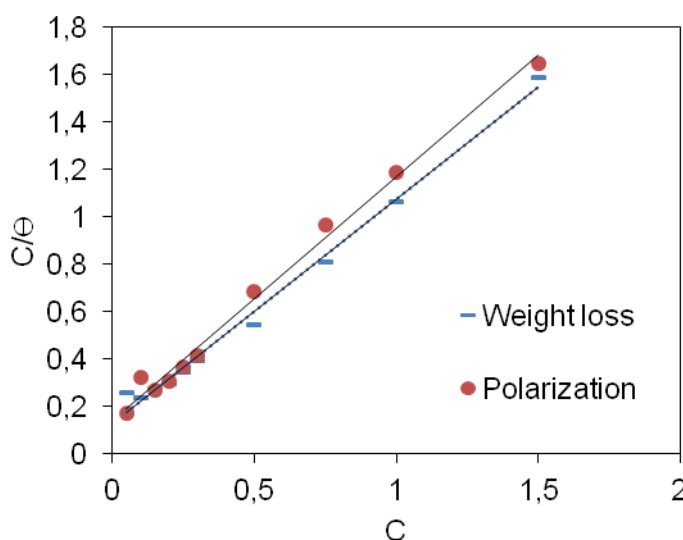


Figure 4. Relationship of C/Θ and Θ for weight loss method and potentiodynamic polarization measurement

The chemisorption process, which is indicated by the values of ΔG_{ads} more negative than -40 kJ mol^{-1} , is attributed to the charge transfer from the molecule or electron sharing between the substrate and other molecules [37]. The calculated parameter from the Langmuir adsorption isotherm fitting (Table 4) indicated the leaf extract to be a mixed-type inhibitor but mainly a physisorption process. This indicated that the extract contained molecules that can adsorb onto the surface of the mild steel by physisorption and chemisorption.

Table 4. Langmuir adsorption isotherm model parameters for the corrosion inhibition measurements of *Aquilaria malaccensis*

Method	R^2	Y-axis intersection	K_{ads}	$\Delta G_{ads} \text{ (kJ mol}^{-1}\text{)}$
Weight loss	0.9922	0.1292	7.73	-22.33
Polarization	0.9922	0.1417	7.05	-22.10
EIS	0.9159	0.3023	3.31	-20.21

3.6. Potential zero charge (PZC) analysis

The potential zero charge (PZC) is the phenomenon when the electric charge density of the surface is zero [38]. The analysis was conducted at the room temperature of $27 \pm 2 \text{ }^\circ\text{C}$. From Fig. 5, the surface net charge of the mild steel can be determined by:

$$E_r = E_{corr} - E_{pzc} \tag{10}$$

where E_r is the Antropov’s “rational” potential (mV) and E_{pzc} is the potential of PZC (mV) where E_{pzc} was taken at the lowest observed conductivity.

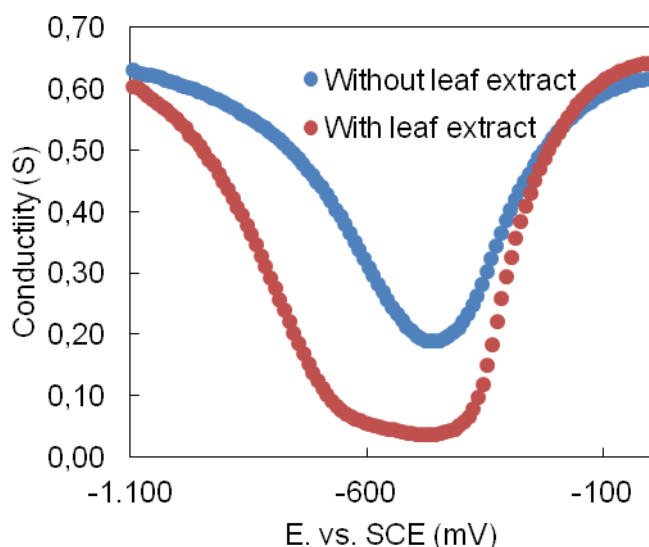


Figure 5. Relationship of conductivity with applied potential for with and without *Aquilaria malaccensis* leaf extract at 1500 ppm at temperature of $27 \pm 2 \text{ }^\circ\text{C}$

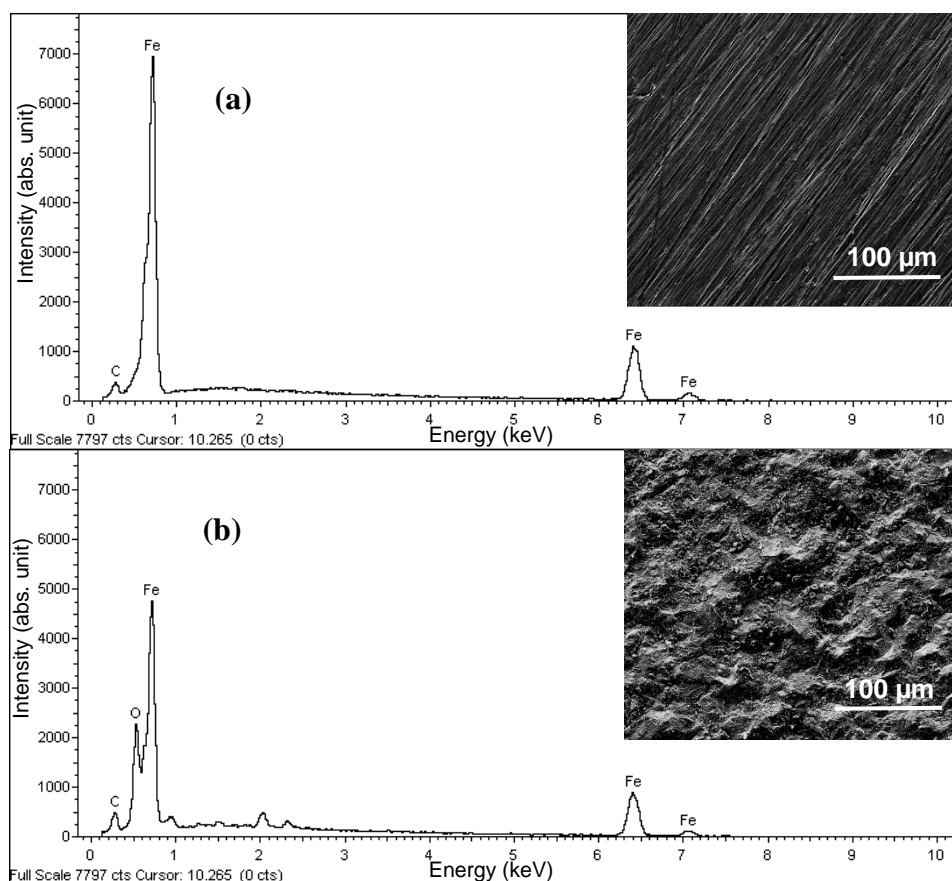
From Table 5, all the values of E_r were positive, indicating that the surfaces of the mild steels were positively charged. A positively charged surface will attract anions, such as the Cl^- (from the HCl) or other anions, from the leaf extract to adsorb over the surface of the mild steel. Some of the molecules in the leaf extract (such as adenosine) can be protonated in the acidic solution, and in turn, be adsorbed on the anion to form a protective thin film over the surface of the mild steel. Aside from this method of physisorption, the molecules could also be chemisorbed as a result of electron transfer/sharing of the valence electron of the functional group or benzene ring on the molecules.

Table 5. Parameters of PZC analysis conducted at temperature of $27 \pm 2 \text{ }^\circ\text{C}$

Specimen	E_{corr} (mV)	E_{PZC} (mV)	E_r (mV)
Without leaf extract	-449	-456	7
With leaf extract	-443	-474	31

3.7. Surface analysis

The SEM images were obtained using a back-scattered electron detector at up to 10 kV and magnification of 1000 \times .



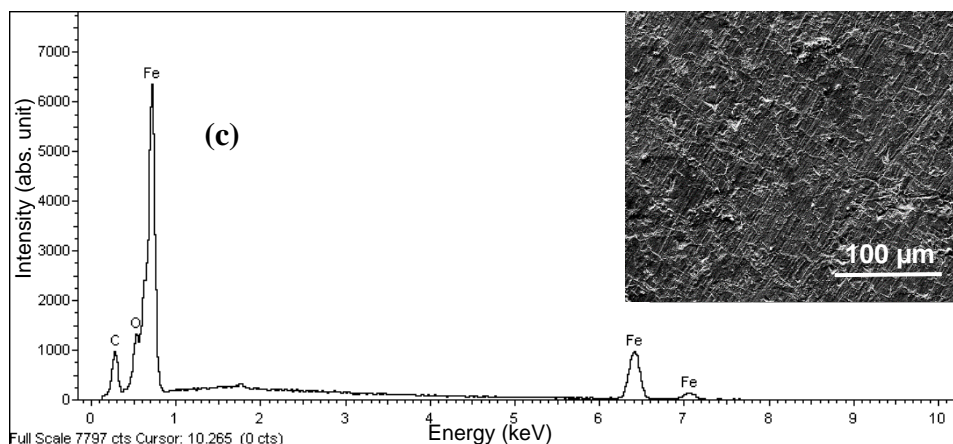


Figure 6. SEM (obtained at up to 10 kV and magnification of 1000× and EDX (inset) of a) polished mild steel, b) mild steel immersed in 1 mol dm⁻³ HCl without *Aquilaria malaccensis* leaf extract, c) mild steel immersed in 1 mol dm⁻³ HCl with *Aquilaria malaccensis* leaf extract

From Fig. 6, the surface of the mild steel immersed in the 1 mol dm⁻³ HCl only is rougher than the surface of the mild steel immersed in the 1 mol dm⁻³ HCl with 1500 ppm of the leaf extract. This indicated a successful corrosion inhibition due to the addition of the leaf extract. The leaf extract formed a protective thin film as a barrier from the corrosive medium, therefore, reducing the effect of corrosion (the roughening) on the surface of the mild steel. This effect of smoother surface of the metal with the presence of successful corrosion inhibitors was observed in several papers [22, 38-41].

The parameters obtained by the surface analysis using EDX are listed in Table 6. From the same table, the O element did not exist in the polished mild steel specimen, indicating a surface that is free from oxidation/corrosion. The surface of the mild steel immersed in the 1 mol dm⁻³ HCl recorded a high intensity of the O element, indicating a formation of corrosive products, which occurred due to the aggressive corrosion reaction in the HCl. The lower O intensity indicated a lower oxidation on the surface of the mild steel immersed with the leaf extract and therefore, the corrosion process on the mild steel was successfully retarded using the leaf extract [39]. The C intensity of the mild steel immersed in the 1 mol dm⁻³ HCl with the leaf extract was almost twice as high as the mild steel immersed in 1 mol dm⁻³ HCl only. This could be attributed to the adsorbed organic molecules from the leaf extract on the surface of the mild steel, thus contributing to the higher intensity of C. This increase in C intensity with the addition of inhibitors was also observed in several papers [39-42].

Table 6. Weight percentage of carbon, oxygen and iron elements on the surface of mild steel immersed for 24 hours at the temperature of 27 ± 2 °C by EDX analysis

Specimen	C (Wt. %)	O (Wt. %)	Fe (Wt. %)
Polished	2.51	-	97.49
Without leaf extract	4.06	8.77	87.17
With leaf extract	7.21	3.89	88.89

4. CONCLUSIONS

- The *Aquilaria malaccensis* leaf extract successfully inhibited the corrosion of mild steel in 1 mol dm⁻³ HCl up to 94.49 % at the concentration of 1500 ppm.
- The leaf extract acted as a mixed-type, but predominantly cathodic inhibitor based on the potentiodynamic polarization measurement.
- The leaf extract was adsorbed by a mixed-type, but predominantly physisorption process based on the Gibbs free energy calculation and the extract best fits the Langmuir adsorption isotherm.
- The surface analysis showed a smoother surface of the mild steel immersed in a 1 mol dm⁻³ solution with the leaf extract compared to that of the blank specimen.

ACKNOWLEDGEMENTS

This study was completed using the financial support in the form of a university grant (1001/PKIMIA/811213). Helen Lee Yun Sin would like to acknowledge the student scholarship provided by MyBrain15 in the form of MyPhD and the Pacific Rim Project from the Nagaoka University of Technology.

References

1. S. Oldfield, C. Lusty, A. MacKinven, The world list of threatened trees, World Conservation Press, 1998.
2. M. Kakino, S. Tazawa, H. Maruyama, K. Tsuruma, Y. Araki, M. Shimazawa, H. Hara, *BMC Complemen. Altern. M.*, 10 (2010) 1.
3. S.L. Li, Y.G. Wang, S.H. Chen, R. Yu, S.B. Lei, H.Y. Ma, D.X. Liu, *Corros. Sci.*, 41 (1999) 1769-1782.
4. A. Braig, *Prog. Org. Coat.*, 34 (1998) 13-20.
5. E.E.F. El Sherbini, *Mater. Chem. Phys.*, 61 (1999) 223-228.
6. P. Mutombo, L. Pospíšil, J. Fiedler, J. Čejka, J. Karhan, J. Vošta, *J. Electroanal. Chem.*, 405 (1996) 223-226.
7. B.A. Abd-El-Nabey, A. El-Toukhy, M. El-Gamal, F. Mahgoob, *Surf. Coat. Tech.*, 27 (1986) 325-334.
8. A. Khadraoui, A. Khelifa, K. Hachama, R. Mehdaoui, *J. Mol. Liq.*, 214 (2016) 293-297.
9. A.N. Grassino, J. Halambek, S. Djaković, S. Rimac Brnčić, M. Dent, Z. Grabarić, *Food Hydrocolloid.*, 52 (2016) 265-274.
10. S. Africa, *Afr. J. Pure Appl. Chem.*, 2 (2008) 046-054.
11. K. Rose, B.-S. Kim, K. Rajagopal, S. Arumugam, K. Devarayan, *J. Mol. Liq.*, 214 (2016) 111-116.
12. N. El Hamdani, R. Fdil, M. Tourabi, C. Jama, F. Bentiss, *Appl. Surf. Sci.*, 357, Part A (2015) 1294-1305.
13. N. Soltani, N. Tavakkoli, M. Khayat Kashani, A. Mosavizadeh, E.E. Oguzie, M.R. Jalali, *J. Ind. Eng. Chem.*, 20 (2014) 3217-3227.
14. M. Mehdipour, B. Ramezanzadeh, S.Y. Arman, *J. Ind. Eng. Chem.*, 21 (2015) 318-327.
15. O.A. Abdullatef, *Egypt. J. Petrol.*, 24 (2015) 505-511.
16. A.Y. El-Etre, M. Abdallah, Z.E. El-Tantawy, *Corros. Sci.*, 47 (2005) 385-395.
17. H. Gerengi, H.I. Sahin, *Ind. Eng. Chem. Res.*, 51 (2011) 780-787.
18. A. Huda, M. Munira, S. Fitrya, M. Salmah, *Pharmacog. Res.*, 1 (2009) 270.

19. A. Khalil, A. Rahim, K. Taha, K. Abdallah, *J. Appl. Ind. Sci.*, 1 (2013) 78-88.
20. L.Y.S. Helen, A.A. Rahim, B. Saad, M.I. Saleh, P.B. Raja, *Int. J. Electrochem. Sci.*, 9 (2014) 830-846.
21. L.Y.S. Helen, A.A. Rahim, C.Y. Gan, B. Saad, M.I. Salleh, M. Umeda, *Measurement, under review*.
22. N. Kıcır, G. Tansuğ, M. Erbil, T. Tüken, *Corros. Sci.*, 105 (2016) 88-99.
23. E.S. Ferreira, C. Giacomelli, F.C. Giacomelli, A. Spinelli, *Mater. Chem. Phys.*, 83 (2004) 129-134.
24. K. Boumhara, M. Tabyaoui, C. Jama, F. Bentiss, *J. Ind. Eng. Chem.*, 29 (2015) 146-155.
25. F. Bentiss, M. Traisnel, L. Gengembre, M. Lagrenée, *Appl. Surf. Sci.*, 152 (1999) 237-249.
26. A. Popova, E. Sokolova, S. Raicheva, M. Christov, *Corros. Sci.*, 45 (2003) 33-58.
27. W.-h. Li, Q. He, S.-t. Zhang, C.-l. Pei, B.-r. Hou, *J. Appl. Electrochem.*, 38 (2007) 289-295.
28. S. Martinez, M. Metikoš-Huković, *J. Appl. Electrochem.*, 33 (2003) 1137-1142.
29. H. Shih, F. Mansfeld, *Corros. Sci.*, 29 (1989) 1235-1240.
30. F. Growcock, R. Jasinski, *J. Electrochem. Soc.*, 136 (1989) 2310-2314.
31. S. Muralidharan, M.A. Quraishi, S.V.K. Iyer, *Corros. Sci.*, 37 (1995) 1739-1750.
32. A. Döner, G. Kardaş, *Corros. Sci.*, 53 (2011) 4223-4232.
33. E.E. Oguzie, *Corros. Sci.*, 49 (2007) 1527-1539.
34. A.J. Bard, L.R. Faulkner, J. Leddy, C.G. Zoski, *Electrochemical methods: fundamentals and applications*, Wiley New York, 1980.
35. M. Lebrini, F. Bentiss, H. Vezin, M. Lagrenée, *Corros. Sci.*, 48 (2006) 1279-1291.
36. T.F. Tadros, *Applied surfactants: principles and applications*, John Wiley & Sons, 2006.
37. E.A. Noor, A.H. Al-Moubaraki, *Mater. Chem. Phys.*, 110 (2008) 145-154.
38. B. Xu, W. Yang, Y. Liu, X. Yin, W. Gong, Y. Chen, *Corros. Sci.*, 78 (2014) 260-268.
39. M. H. Hussin, A. A. Rahim, M. N. M. Ibrahim, N. Brosse, *Measurement*, 78 (2016) 90-103.
40. M. Yadav, S. Kumar, R. R. Sinha, I. Bahadur, E. E. Ebenso, *J. Mol. Liq.*, 211 (2015) 135-145.
41. M. Yadav, R. R. Sinha, T. K. Sarkar, I. Bahadur, *J. Mol. Liq.*, 212 (2015) 686-698.
42. M. A. Amin, S. S. A. El-Rehim, E. E. F. El-Sherbini, R. S. Bayoumi, *Electrochim. Acta*, 52 (2007) 3588-3600.